Accepted Manuscript

New racemic annulated pyrazolo[1,2-*b*]phthalazines as tacrine-like AChE inhibitors with potential use in Alzheimer's disease

Leili Jalili-Baleh, Hamid Nadri, Alireza Moradi, Syed Nasir Abbas Burkhart, Mojtaba Shakibaie, Mandana Jafari, Mostafa Golshani, Farshad Homayouni Moghadam, Loghman Firoozpour, Ali Asadipour, Saeed Emami, Mehdi Khoobi, Alireza Foroumadi

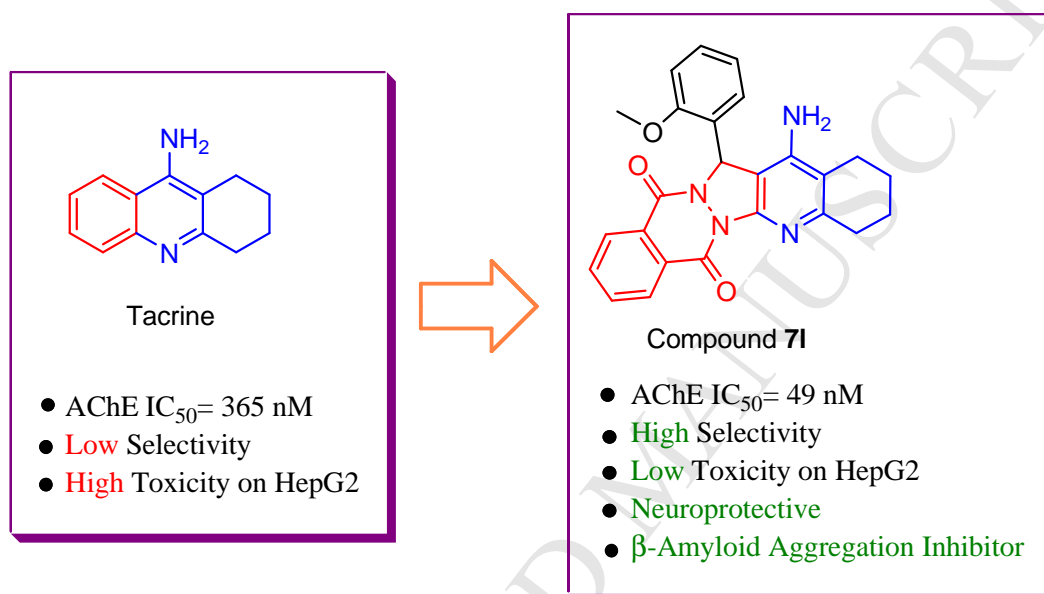Please cite this article as: L. Jalili-Baleh, H. Nadri, A. Moradi, S.N. Abbas Burkhart, M. Shakibaie, M. Jafari, M. Golshani, F.H. Moghadam, L. Firoozpour, A. Asadipour, S. Emami, M. Khoobi, A. Foroumadi, New racemic annulated pyrazolo[1,2-*b*]phthalazines as tacrine-like AChE inhibitors with potential use in Alzheimer's disease, *European Journal of Medicinal Chemistry* (2017), doi: 10.1016/j.ejmech.2017.07.072.

Graphical abstract

New racemic annulated pyrazolo[1,2-_b_]phthalazines as tacrine-like AChE inhibitors with potential use in Alzheimer's disease

Leili Jalili-Baleh, Hamid Nadri, Alireza Moradi, Syed Nasir Abbas Burkhart, Mojtaba Shakibaie, Mandana Jafari, Mostafa Golshani, Farshad Homayouni Moghadam, Loghman Firoozpour, Ali Asadipour, Saeed Emami, Mehdi Khoobi, Alireza Foroumadi

Tacrine

- AChE IC$_{50}$= 365 nM
- Low Selectivity
- High Toxicity on HepG2

Compound **7I**

- AChE IC$_{50}$= 49 nM
- High Selectivity
- Low Toxicity on HepG2
- Neuroprotective
- β-Amyloid Aggregation Inhibitor

A series of tacrine-like compounds **7a-u** were designed and synthesized as potent AChE inhibitors with high selectivity, low toxicity on hepatocytes, neuroprotective and and β-amyloid aggregation inhibitory activity.

New racemic annulated pyrazolo[1,2-*b*]phthalazines as tacrine-like AChE inhibitors with potential use in Alzheimer's disease

Leili Jalili-Baleh [a], Hamid Nadri [b], Alireza Moradi [b], Syed Nasir Abbas Burkhart [c], Mojtaba Shakibaie [d], Mandana Jafari [d], Mostafa Golshani [a], Farshad Homayouni Moghadam [e], Loghman Firoozpour [f], Ali Asadipour [g], Saeed Emami [h], Mehdi Khoobi [a,i]*, Alireza Foroumadi [a,g]**

[a]*Department of Medicinal Chemistry, Faculty of Pharmacy and Pharmaceutical Sciences Research Center, Tehran University of Medical Sciences, Tehran, Iran*

[b]*Faculty of Pharmacy, Shahid Sadoughi University of Medical Sciences, Yazd, Iran*

[c]*Department of Pharmaceutical Chemistry, College of Pharmacy, Aljouf University, Aljouf, Sakaka 2014, Saudi Arabia*

[d]*Pharmaceutics Research Center, Institute of Neuropharmacology, Kerman University of Medical Sciences, Kerman, Iran*

[e]*Department of Cellular Biotechnology, Cell Science Research Center, Royan Institute for Biotechnology, ACECR, Isfahan, Iran*

[f]*Drug Design and Development Research Center, Tehran University of Medical Sciences, Tehran, Iran*

[g]*Department of Medicinal Chemistry, Faculty of Pharmacy and Neuroscience Research Center, Institute of Neuropharmacology, Kerman University of Medical Sciences, Kerman, Iran*

[h]*Department of Medicinal Chemistry and Pharmaceutical Sciences Research Center, Faculty of Pharmacy, Mazandaran University of Medical Sciences, Sari, Iran*

[i]*Department of Pharmaceutical Biomaterials and Medical Biomaterials Research Center, Faculty of Pharmacy, Tehran University of Medical Sciences, Tehran, Iran*

Abstract: A novel series of tacrine-like compounds **7a-u** possessing a fused pyrazolo[1,2-*b*]phthalazine structure were designed and synthesized as potent and selective inhibitors of AChE. The in-vitro biological assessments demonstrated that several compounds had high anti-AChE activity at nano-molar level. The more promising compound **7l** with IC_{50} of 49 nM was 7-fold more potent than tacrine and unlike tacrine, it was highly selective against AChE over BuChE. The cell-based assays against hepatocytes (HepG2) and neuronal cell line (PC12) revealed that **7l** had significantly lower hepatotoxicity compared to tacrine, with additional neuroprotective activity against H_2O_2-induced damage in PC12 cells. This compound could also inhibit AChE-induced and self-induced Aβ peptide aggregation. The advantages including synthetic accessibility, high potency and selectivity, low toxicity, adjunctive neuroprotective and Aβ aggregation inhibitory activity, make this compound as a new multifunctional lead for Alzheimer's disease drug discovery.

* Corresponding author. Tel/Fax: +98-21-64121113. E-mail address: Mehdi.khoobi@gmail.com (M. Khoobi)
** Corresponding authors: Tel: +98-21-66954708; Fax: +98 21 66461178. E-mail addresses: aforoumadi@yahoo.com (A. Foroumadi)

1. Introduction

Alzheimer's disease (AD) as a most common cause of dementia is a neurodegenerative disorder with complex pathological mechanisms. World health organization (WHO) predicted that over the next century AD will be more prevalent than AIDS, cancer and cardiovascular diseases [1]. The most important factors involved in AD are acetylcholine (ACh) decline, accumulation of insoluble forms of amyloid-β (Aβ) and the hyperphosphorylated tau protein followed by inflammatory actions [2].

Because of multi-factorial nature of AD, and despite extensive research for understanding the mechanism of the disease, development of new therapeutics is still challenging [3]. In particular, design of multi-target directed ligands which act on multiple pathophysiological pathways of AD has gained special attention [4, 5]. The main approved AD therapy has been focused on increasing cholinergic transmission by inhibition of acetylcholinesterase (AChE) and butyrylcholinesterase (BuChE) enzymes [6, 7]. By inhibiting cholinesterases, the amount of ACh is enhanced in the neuronal synaptic cleft. Besides of cholinergic hypothesis, it was approved that the peripheral anionic site (PAS) of AChE contributes to aggregation of amyloid fibrils [8]. Also, recent evidences demonstrated that oxidative damage is an early occurrence in initial progress of the neurodegenerative process in AD pathology [9, 10]. Therefore, protection against oxidative stress by neuroprotective agents will be a suitable additional therapy for AD [11].

Tacrine, an aminoacridine derivative (Fig. 1, **A**), was the first AChE inhibitor approved for treatment of AD [12, 13]. This compound was withdrawn from the market due to its hepatotoxicity [14]. In spite of tacrine's side effects, it is still an attractive lead compound for medicinal chemists due to its synthetic accessibility, low molecular weight and relatively easy modification [15]. To develop new less toxic tacrine derivatives with high anticholinesterase and selective peripheral binding potency, the replacement of benzene ring in the tacrine structure with different heterocyclic systems has been considered more extensively [16, 17]. Previously, we described a number of pyrazolo[4′,3′:5,6]pyrano[2,3-*b*]quinolines as novel

tacrine-derived AChE inhibitors [18, 19]. Furthermore, Barreiro et al. have reported a series of tacrine-like compounds containing pyrazolo-quinoline scaffold (Fig.1). The rat brain cholinesterases inhibition assay revealed that compound **B** (Fig.1) had the most potent AChE inhibitory activity [20]. On the other hand, some phthalazinone derivatives were also synthesized and evaluated for their AChE and BuChE inhibitory activities [21-24].

In the light of above-mentioned reports, we were encouraged to design and synthesize a novel series of tacrine-based compounds through replacement of the benzene ring in tacrine with pyrazolo[1,2-*b*]phthalazine scaffold (Fig. 1). Thus we describe here the synthesis, in vitro and in silico studies of compounds **7a-u** as multifunctional agents for AD therapy.

2. Chemistry

The straightforward synthetic route to target compounds **7a-u** was illustrated in Scheme 1. The key intermediates pyrazolo[1,2-*b*]phthalazines **5a-u** was synthesized via multi-component reaction of phthalimide (**1**), hydrazine hydrate (**2**), malononitrile (**3**) and appropriate benzaldehyde derivative **4** in the presence of $NiCl_2 \cdot 6H_2O$ as catalyst in refluxing ethanol [25]. The pyrazolo[1,2-*b*]phthalazines **5** underwent $AlCl_3$-catalyzed Friedländer cyclization with cyclohexanone (**6**) to obtain final products **7a-u** [26].

3. Results and discussion

3.1. Anti-cholinesterase activity and SAR discussion

The synthesized tacrine-like compounds **7a-u** were evaluated in vitro for their anti-cholinesterase activity against AChE and BuChE in comparison to tacrine as reference drug. The obtained IC_{50} values of compounds **7a-u** against AChE and BuChE were presented in Table 1. In general, all compounds exhibited potent activity against AChE (IC_{50} values ≤3.37 µM). Notably, compounds **7b-d**, **7l** and **7o** possessing IC_{50} values in the range of 23-80 nM were several times more potent than tacrine. The 3-fluorophenyl derivative **7o** was the most potent compound against AChE being 15-fold more potent than tacrine.

The IC_{50} values of 4-substituted phenyl derivatives **7b-f** were less than that of unsubstituted analog **7a**. Thus, introduction of substituents such as halogen, Me and NO_2 at the *para*-position improves the anti-AChE activity. However, halogen group at the *para*-position of phenyl ring is more favorable than other substituents. Although the substitution of halo group at *ortho*-position of phenyl ring could not improve inhibitory activity, but insertion of 2-Me, 2-NO_2 and 2-MeO had positive effect on anti-AChE potency. In particular, 2-methoxyphenyl analog **7l** showed high potency with IC_{50} of 49 nM. Also, the *meta*-substituent on the phenyl ring could positively modulate the inhibitory potential against AChE. However, introduction of additional methoxy group at meta (3,5-dimethoxy) led to decrease of the activity against AChE. The effect of 3-F substituent was more significant as observed with compound **7o** as the most potent derivative in the series.

Based on the results gathered in the Table 1, the anti-AChE potency was significantly affected by the substitution on the C-14 of the pentacyclic framework. Replacing the 14-aryl moiety with aliphatic groups such as methyl and propyl decreased the activity. However, the pentyl derivative **7u** was as potent as unsubstituted-phenyl analog **7a**.

As observed in Table 1, most of compounds were inactive against BuChE enzyme (IC_{50}s >100 µM). However, the most potent compound against AChE (**7o**), showed mild activity against BuChE (IC_{50}= 37.2 µM). Unlike tacrine, all compounds exhibited high selectivity for AChE over BuChE.

3.2. Kinetic study of AChE inhibition

The kinetics of AChE inhibition was studied for the active compound **7l** with IC_{50} value of 49 nM. For this purpose, the rate of AChE inhibition by different concentrations (0, 25, 50 and 100 nM) of the potent inhibitor **7l** was measured in the presence of substrate (ATCh). The cholinesterase inhibition was determined as described in the experimental section. For each inhibitor concentration, the initial velocity was measured at different substrate concentrations (S) and the reciprocal of the initial velocity (1/v) was plotted respect to the reciprocal of substrate concentration (1/[S]). Accordingly, the Lineweavere-Burk plot for the inhibition of AChE and the secondary plot for calculation of steady-state inhibition constant (K_i) for compound **7l** were illustrated in Fig. 2. The Lineweavere-Burk plot showed a mixed-type

inhibition pattern for compound **7l** against AChE. The K_i value was 12.64 nM as calculated from the secondary plot in Fig. 2.

3.3. Inhibition of AChE-induced and self-induced Aβ aggregation

Compound **7l** as a potent AChE inhibitor was selected to assess its ability to inhibit $Aβ_{1-42}$ peptide self-aggregation employing the thioflavin T (ThT) fluorescence method and compared with donepezil as reference compound. The obtained inhibition for compound **7l** at 10 μM concentration was 25.5% being higher than that of donepezil (15.4%, Table 2). To further explore the dual action of this compound, the capacity to inhibit the AChE-induced $Aβ_{1-40}$ peptide aggregation was examined employing the same ThT-based fluorometric assay. As seen in Table 2, compound **7l** exhibited a significant AChE-induced Aβ aggregation inhibitory effect with percentage of inhibition 32% more effective than tacrine and donepezil, indicating that compound **7l** binds to PAS of AChE.

3.4. Cytotoxicity on HepG2 cells

As described in the Introduction section, the well-known drug tacrine suffers from hepatotoxicity [14]. Thus, the tacrine-derived compounds may be associated with the cytotoxicity on hepatocytes [27, 28]. In order to verify the hepatotoxicity of the selected compounds (**7b-d, 7l** and **7o**), an in vitro cytotoxicity assay was conducted on HepG2 cell line. The effect of selected compounds on the viability of HepG2 cells at different concentrations was outlined in Table 3. The obtained results showed that the cytotoxicity of all tested compounds was significantly lower than that of tacrine. Particularly, 4-bromophenyl derivative **7c** showed no significant cytotoxicity even at the concentration of 50 μM. However, tacrine decreased the cell viability to 66.4% at this concentration. The 4-fluoro- and 3-fluoro-phenyl analogs (**7d** and **7o**, respectively) were somehow more toxic than 4-chloro-, 4-bromo- and 2-methoxy-phenyl derivatives (**7b**, **7c** and **7l**).

3.5. Neuroprotective activity of compound 7l against H₂O₂-induced cell death in PC12 cells

Besides cholinesterases inhibition, other strategies such as protection against oxidative stress may be useful in the management of AD [29]. Thus, the capability of the representative compound **7l** in the protection of neuronal cell line PC12 against H_2O_2-induced damage was investigated in vitro. The differentiated PC12 cells were treated with compound **7l** at the concentrations of 1, 10 and 100 µM, prior to treatment with H_2O_2 (375 µM). The cell viability was measured in comparison to quercetin by using MTT assay and the obtained results were depicted in Fig. 3. As seen in Fig. 3, compound **7l** (100 µM) significantly increased the viability of PC12 cells under the ROS-mediated apoptosis condition. The neuroprotective activity of compound **7l** at 100 µM was comparable to quercetin (10 µM). It should be noted that compound **7l** at the 1 and 10 µM concentrations was neither neurotoxic nor neuroprotective.

3.6. ADMET prediction

The ADMET (absorption, distribution, metabolism, excretion and toxicity) properties of the target compounds **7a-u** were predicted using admetSAR web-based application [30]. Based on the predicted values (Table 4), all compounds are able to penetrate brain with a probability of more than 90%, therefore they are considered as CNS-active compounds. Moreover, all compounds were predicted to have no carcinogenic effect. Finally all compounds were examined for oral activity using HIA and Caco-2 method. It was revealed that all compounds may show desired oral absorption.

3.7. Ligand-protein docking study

The most promising compound **7l** was selected for docking study with acetylcholinesterase (1EVE) by using the AutoDock software. Since compound **7l** have a chiral center at the 14-position of pyrazoline ring, they are racemic mixture. Thus, both (*R*)- and (*S*)-enantiomers were studied in docking simulations. The binding energy of (*S*)-enantiomer was low and the interactions were unfavorable but the (*R*)-enantiomer was fitted well in the active site. As depicted in Figs 4 and 5, compound **7l** is positioned in the enzyme active site in such a way to interact with the amino acids at the rim of the cavity, and to act as a barrier preventing the

6

entry of the substrates into the active site. The fused-rings part of the compound, which has an approximately planar structure, makes π-π stacking with the aromatic amino acids at the rim of the active site (PAS) including tyrosine 120 and tryptophan 278. Moreover, the cyclohexene ring binds to tryptophan 278 by a π-alkyl interaction. In this situation, one carbonyl group along with nitrogen of the pyridine ring bind to the hydroxyl group of tyrosine 69 by forming a network of hydrogen bonds. The pendent aryl group connected to 14-position of the fused rings is positioned almost perpendicularly to the plane of the fused rings and forms an intramolecular bond with the amine group.

4. Conclusion

A multi-component reaction followed by Friedländer reaction were applied to prepare a novel tacrine analogs **7a-u** bearing pyrazolo[1,2-*b*]phthalazines as selective anti-acetycholinesterase agents. The anti-AChE activity of the designed compounds was optimized through altering the pendent group on C-14 position of the pentacyclic skeleton. Most of compounds showed selective anti-AChE activity at sub-micromolar levels. The best result was obtained by 3-fluorophenyl in compound **7o** with IC_{50} of 23 nM against AChE. This compound was 15 times more potent than tacrine against AChE. Besides compound **7o**, the 2-methoxyphenyl derivative **7l** with IC_{50} of 49 nM showed high potency against AChE. The promising compounds **7o** and **7l** were highly selective for AChE over BuChE, and significantly less toxic than reference drug tacrine. Since compound **7l** showed less cytotoxic effect on HepG2 cells, thus this compound was selected for further studies. The biological results indicated that compound **7l** had neuroprotective activity against H_2O_2-induced damage in PC12 cells at higher concentrations. Moreover, compound **7l** was found to be an inhibitor of AChE-induced Aβ aggregation, which can also interfere with Aβ self-aggregation. The docking study of compound **7l** with AChE enzyme revealed that the fused rings component of the molecule made π-π stacking with the aromatic amino acids at the peripheral anionic site of the enzyme (PAS). The straightforward synthesis, high potency and selectivity against AChE, inhibition of AChE-induced Aβ aggregation as well as Aβ self-aggregation, relatively low toxicity, along with significant neuroprotective effects of newly designed tacrine-like

7

compounds **7a-u** introduce them as attractive lead compounds towards discovery of effective disease-modifying drugs for AD therapy.

5. Experimental

5.1. General chemistry

All commercially available reagents and starting materials were used without further purification. TLC was conducted on silica gel 250 micron, F254 plates (Merck). Melting points were measured on a Kofler hot stage apparatus and are uncorrected. The IR spectra were taken using Nicolet FT-IR Magna 550 spectrograph (KBr disks). ^{1}H NMR spectra were recorded on Brucker 500 MHz NMR instrument. The chemical shifts (δ) and coupling constants (J) are presented in parts per million (ppm) and Hertz (Hz), respectively. Scheme 1 shows the atoms numbering of the final compounds **7a**-**u** useful in the ^{1}H NMR interpretation. Elemental analyses were carried out by a CHN-Rapid Heraeus Elemental Analyzer. The results of elemental analyses (C, H, N) were within ±0.4% of the calculated values.

5.2. General procedure for the preparation of pyrazolo[1,2-b]phthalazine derivatives *5a-u*

This procedure was carried out according to the reported method [25]. A mixture of phthalimide (**1**, 1 mmol), hydrazine hydrate (**2**, 1 mmol) and NiCl$_2$ .6H$_2$O (0.1 mmol) in ethanol (3 mL) was refluxed for 2 h. Afterward, malononitrile (**3**, 1 mmol) and approperiate aldehyde (1 mmol) were added and the mixture was refluxed for 2 h. The precipitated solid was separated by filtration and recrystallized from ethanol to obtain pure product **5a-u**.

5.3. General procedure for the preparation of compounds *7a-u*

This procedure was carried out according to our previously reported method [26]. Briefly, aluminium chloride (1.5 equiv.) was suspended in dry 1,2-dichloroethane (10 mL) at room temperature under argon atmosphere. After stirring of the suspension for a few minutes, the corresponding pyrazolo[1,2-*b*]phthalazine (**5**, 1 equiv.) and cyclohexanone (**6**, 1.5 equiv.) were added to the mixture and the reaction mixture was heated under

reflux for 24 h. Progress of the reaction was monitored by TLC. After completion of the reaction, an aqueous saturated solution of ammonium chloride was added to the mixture until the aqueous solution became basic. After stirring for 30 min, the precipitate was filtered, washed with water and recrystallized with acetonitrile.

5.3.1.   15-Amino-14-phenyl-2,3,4,14-tetrahydro-1H-quinolino[2',3':3,4]pyrazolo[1,2-b]phthalazine-7,12-dione (7a). Yield 90%; off white solid; mp >250 ºC; IR (KBr, cm^{-1}) ν_{max}: 3421 and 3373 (NH$_2$), 1642 (C=O), 1581 (C=N). ^{1}H NMR (DMSO-d_6, 500 MHz) δ: 8.28 (d, 1H, J = 7.5 Hz, H$_8$ phthalazine), 8.01 (d, 1H, J = 7.5 Hz, H$_{11}$ phthalazine), 7.91 (m, 2H, H$_{9,10}$ phthalazine), 7.44 (d, 2H, J = 7.5 Hz, H$_{2,6}$ phenyl), 7.28 (m, 3H, H$_{3,4,5}$ phenyl), 6.73 (s, 1H, H$_{14}$), 5.63 (S, 2H, NH$_2$), 2.73 (bs, 2H, cyclohexyl), 2.39-2.26 (m, 2H, cyclohexyl), 1.75 (bs, 4H, cyclohexyl). ^{13}C NMR (DMSO-d_6, 100 MHz) δ: 155.35, 153.5, 152.7, 148.3, 147.7, 137.5, 133.46, 133.34, 130.2, 128.19, 127.92, 127.36, 127.28, 126.44, 113.8, 100.2, 95.32, 61.08, 32.6, 22.3, 21.86. Anal. Calcd for C$_{24}$H$_{20}$N$_4$O$_2$: C, 72.1; H, 5.09; N, 14.13. Found: C, 72.53; H, 6.93; N, 15.01.

5.3.2.   15-Amino-14-(4-chlorophenyl)-2,3,4,14-tetrahydro-1H quinolino[2',3':3,4]pyrazolo[1,2-b]phthalazine-7,12-dione (7b). Yield 85%; off white solid; mp >250 ºC; IR (KBr, cm^{-1}) ν_{max}: 3421 and 3373 (NH$_2$), 1629 (C=O), 1581 (C=N). ^{1}H NMR (DMSO-d_6, 500 MHz) δ: 8.45 (d, 1H, J = 7.3 Hz, H$_8$ phthalazine), 8.24 (d, 1H, J = 7.4 Hz, H$_{11}$ phthalazine), 7.82 (m, 2H, H$_{9,10}$ phthalazine), 7.46 (d, 2H, J = 8.05 Hz, H$_{2,6}$ phenyl), 7.35 (d, 2H, J = 7.95 Hz, H$_{3,4,5}$ phenyl), 6.6 (s, 1H, H$_{14}$), 4.3 (S, 2H, NH$_2$), 3.0 (bs, 2H, cyclohexyl), 2.23 (bs, 2H, cyclohexyl), 1.85 (bs, 4H, cyclohexyl). ^{13}C NMR (DMSO-d_6, 100 MHz) δ: 155.6, 153.5, 152.6, 148.4, 147.8, 147.71, 136.9, 133.6, 133.5, 131.2, 130.2, 129.9, 128.2, 127.4, 126.5, 121.3, 113.8, 101.5, 60.6, 45.1, 32.7, 22.8, 22.3, 21.9. Anal. Calcd for C$_{24}$H$_{19}$ClN$_4$O$_2$: C, 66.9; H, 4.44; N, 13. Found: C, 66.02; H, 3.9; N, 14.01.

5.3.3.   15-Amino-14-(4-bromophenyl)-2,3,4,14-tetrahydro-1H-quinolino[2',3':3,4]pyrazolo[1,2-b]phthalazine-7,12-dione (7c). Yield 90%; off white solid; mp >250 ºC; IR (KBr, cm^{-1}) ν_{max}: 3461 and 3394 (NH$_2$), 1626 (C=O), 1500 (C=N). ^{1}H

NMR (DMSO-d_6, 500 MHz) δ: 8.27 (d, 1H, J = 7.4 Hz, H$_8$ phthalazine), 8.08 (d, 1H, J = 6.8 Hz, H$_{11}$ phthalazine), 7.93 (m, 2H, H$_{9,10}$ phthalazine), 7.49 (d, 2H, J = 7.6 Hz, H$_{2,6}$ phenyl), 7.42 (d, (d, 2H, J = 7.7 Hz, H$_{3,5}$ phenyl), 6.7 (s, 1H, H$_{14}$), 5.7 (S, 2H, NH$_2$), 2.73 (bs, 2H, cyclohexyl), 2.40-2.26 (m, 2H, cyclohexyl), 1.75 (bs, 4H, cyclohexyl). ^{13}C NMR (DMSO-d_6, 100 MHz) δ:155.51, 153.47, 152.55, 148.34, 147.76, 136.73, 133.46, 133.38, 131.08, 130.14, 129.77, 128.15, 127.28, 126.43, 121.18, 113.83, 101.35, 60.48, 44.88, 32.59, 22.74, 22.27, 21.85. Anal. Calcd for C$_{24}$H$_{19}$BrN$_4$O$_2$: C, 66.64; H, 4.03; N, 11.79. Found: C, 66.12; H, 3.95; N, 11.11.

5.3.4. *15-Amino-14-(4-fluorophenyl)-2,3,4,14-tetrahydro-1H-quinolino[2',3':3,4]pyrazolo[1,2-b]phthalazine-7,12-dione (7d).* Yield 92%; off white solid; mp >300 ºC; IR (KBr, cm^{-1}) ν_{max}: 3454 and 3421 (NH$_2$), 1633 (C=O), 1507 (C=N). ^{1}H NMR (DMSO-d_6, 500 MHz) δ: 8.27 (d, 1H, J = 8 Hz, H$_8$ phthalazine), 8.1 (d, 1H, J = 7 Hz, H$_{11}$ phthalazine), 7.9 (m, 2H, H$_{9,10}$ phthalazine), 7.48 (m, 2H, H$_{2,6}$ phenyl), 7.1 (t, 2H, J = 9 Hz, H$_{3,4,5}$ phenyl), 6.75 (s, 1H, H$_{14}$), 5.65 (S, 2H, NH$_2$), 2.73 (bs, 2H, cyclohexyl), 2.4-2.27 (m, 2H, cyclohexyl), 1.76 (bs, 4H, cyclohexyl). ^{13}C NMR (DMSO-d_6, 100 MHz) δ: 155.47, 153.46, 152.58, 148.4, 147.76, 147.2, 133.48, 133.37, 130.13, 129.77, 129.71, 128.22, 127.28, 126.44, 115.02, 114.85, 113.81, 101.56, 60.37, 32.60, 22.75, 22.28, 21.86. Anal. Calcd for C$_{24}$H$_{19}$FN$_4$O$_2$: C, 69.55; H, 4.62; N, 13.52. Found: C, 69.41; H, 4.43; N, 13.51.

5.3.5. *15-Amino-14-(p-tolyl)-2,3,4,14-tetrahydro-1H-quinolino[2',3':3,4]pyrazolo[1,2-b]phthalazine-7,12-dione (7e).* Yield 95%; off white solid; mp >250 ºC; IR (KBr, cm^{-1}) ν_{max}: 3446 and 3360 (NH$_2$), 1632 (C=O), 1490 (C=N). ^{1}H NMR (DMSO-d_6, 500 MHz) δ: 8.28 (d, 1H, J = 7.5 Hz, H$_8$ phthalazine), 8.08 (d, 1H, J = 7 Hz, H$_{11}$ phthalazine), 7.9 (m, 2H, H$_{9,10}$ phthalazine), 7.3 (d, 2H, J = 7.5 Hz, H$_{2,6}$ phenyl), 7.08 (d, 2H, J = 7.5 Hz, H$_{3,5}$ phenyl), 6.69 (s, 1H, H$_{14}$), 5.58 (S, 2H, NH$_2$), 2.73 (bs, 2H, cyclohexyl), 2.42-2.29 (bs, 2H, cyclohexyl), 2.23 (bs, 3H, Me), 1.75 (bs, 4H, cyclohexyl). ^{13}C NMR (DMSO-d_6, 100 MHz) δ: 155.30, 153.35, 152.54, 148.29, 147.67, 137.29, 134.46, 133.46, 133.31, 130.07, 128.75, 128.29, 127.35, 127.26, 126.42, 113.77, 101.94, 60.91, 32.58, 22.74, 22.30, 21.88, 20.55. Anal. Calcd for C$_{25}$H$_{22}$N$_4$O$_2$: C, 73.15; H, 5.40; N, 13.65. Found: C, 72.95; H, 4.80; N, 13.33.

5.3.6. *15-Amino-14-(4-nitrophenyl)-2,3,4,14-tetrahydro-1H-quinolino[2',3':3,4]pyrazolo[1,2-b]phthalazine-7,12-dione (7f).* Yield 80%; off white solid; mp >250 ºC; IR (KBr, cm^{-1}) ν_{max}: 3435 and 3358 (NH$_2$), 1633 (C=O), 1530 (C=N). ^{1}H NMR (DMSO-d_6, 500 MHz) δ: 8.28-7.9 (m, 6H, H$_{8,9,10,11}$ phthalazine, H$_{2,6}$ phenyl), 7.7 (t, 2H, J = 8.5 Hz, H$_{3,5}$ phenyl), 6.8 (s, 1H, H$_{14}$), 5.7 (s, 2H, NH$_2$), 2.73 (bs, 2H, cyclohexyl), 2.40-2.23 (m, 2H, cyclohexyl), 1.75 (bs, 4H, cyclohexyl). ^{13}C NMR (DMSO-d_6, 100 MHz) δ: 156.97, 155.76, 150.85, 148.42, 147.90, 147.12, 134.57, 133.73, 133.53, 130.25, 128.88, 127.99, 127.35, 126.62, 123.67, 123.40, 113.97, 101.03, 60.40, 32.61, 22.77, 22.25, 21.83. Anal. Calcd for C$_{24}$H$_{19}$N$_5$O$_4$: C, 65.30; H, 4.34; N, 15.86. Found: C, 66.08; H, 4.35; N, 14.91.

5.3.7. *15-Amino-14-(2-chlorophenyl)-2,3,4,14-tetrahydro-1H-quinolino[2',3':3,4]pyrazolo[1,2-b]phthalazine-7,12-dione (7g).* Yield 80%; off white solid; mp >250 ºC; IR (KBr, cm^{-1}) ν_{max}: 3472 and 3410 (NH$_2$), 1661 (C=O), 1556 (C=N). ^{1}H NMR (DMSO-d_6, 500 MHz) δ: 8.34 (d, 1H, H$_8$ phthalazine), 8.15 (d, 1H, H$_{11}$ phthalazine), 8.04-7.96 (m, 2H, 2H$_{9,10}$ phthalazine), 7.88 (1H, H$_3$ phenyl), 7.43 (m, 3H, H$_{4,5,6}$ phenyl), 7.03 (s, 1H, H$_{14}$), 6.9 (S, 2H, NH$_2$), 2.92 (bs, 2H, cyclohexyl), 2.47-2.30 (m, 2H, cyclohexyl), 1.75 (bs, 4H, cyclohexyl). ^{13}C NMR (DMSO-d_6, 100 MHz) δ: 154.35, 135.79, 134.64, 134.01, 132.55, 131.34, 130.53, 130.6, 130.42, 127.51, 127.44, 126.89, 114.97, 100.83, 61.48, 22.59, 22.50, 21.19, 21.00. Anal. Calcd for C$_{24}$H$_{19}$ClN$_4$O$_2$: C, 66.90; H, 4.44; N, 13. Found: C, 65.93; H, 4.63; N, 13.81.

5.3.8. *15-Amino-14-(2-bromophenyl)-2,3,4,14-tetrahydro-1H-quinolino[2',3':3,4]pyrazolo[1,2-b]phthalazine-7,12-dione (7h).* Yield 85%; off white solid; mp >250 ºC; IR (KBr, cm^{-1}) ν_{max}: 3424 and 3360 (NH$_2$), 1638 (C=O), 1496 (C=N). ^{1}H NMR (DMSO-d_6, 500 MHz) δ: 8.31 (d, 1H, J = 7.5 Hz, H$_8$ phthalazine), 8.07 (d, 1H, J = 67.5 Hz, H$_{11}$ phthalazine), 7.95 (m, 1H, H$_3$ phenyl), 7.88 (m, 2H, H$_{9,10}$ phthalazine), 7.60 (d, 1H, H$_5$ phenyl), 7.37 (t, 1H, J = 7 Hz, H$_6$ phenyl), 7.24 (td, 1H, J = 8 Hz, H$_4$ phenyl), 6.85 (s, 1H, H$_{14}$), 5.2 (S, 2H, NH$_2$), 2.73 (bs, 2H, cyclohexyl), 2.39-2.27 (m, 2H, cyclohexyl), 1.75 (bs, 4H, cyclohexyl). ^{13}C NMR (DMSO-d_6, 100 MHz) δ: 155.73, 153.74, 152.77, 148.57, 135.53, 133.55, 133.20, 132.49, 130.26, 130.18, 128.36, 172.93, 127,

35, 126.44, 113.98, 62.25, 32.57, 22.7, 22.24, 21.8. Anal. Calcd for $C_{24}H_{19}BrN_4O_2$: C, 60.64; H, 4.03; N, 11.79. Found: C, 61.38; H, 4.79; N, 10.11.

5.3.9. *15-Amino-14-(2-fluorophenyl)-2,3,4,14-tetrahydro-1H-quinolino[2',3':3,4]pyrazolo[1,2-b]phthalazine-7,12-dione (7i).* Yield 80%; off white solid; mp >250 ℃; IR (KBr, cm^{-1}) ν_{max}: 3478 and 3356 (NH$_2$), 1658 (C=O), 1530 (C=N). ^{1}H NMR (DMSO-d_6, 500 MHz) δ: 8.31 (d, 1H, J = 7.5 Hz, H$_8$ phthalazine), 8.08 (d, 1H, J = 7.5 Hz, H$_{11}$ phthalazine), 7.94 (m, 1H, H$_3$ phenyl), 7.88 (m, 2H, H$_{9,10}$ phthalazine), 7.33 (t, 1H, J = 7 Hz, H$_5$ phenyl), 7.19 (t, 1H, J = 8 Hz, H$_6$ phenyl), 7.07 (t, 1H, J = 8 Hz, H$_4$ phenyl), 6.8 (s, 1H, H$_{14}$), 5.53 (s, 2H, NH$_2$), 2.72 (bs, 2H, cyclohexyl), 2.4-2.26 (m, 2H, cyclohexyl), 1.75 (bs, 4H, cyclohexyl). ^{13}C NMR (DMSO-d_6, 100 MHz) δ: 155.51, 152.63, 152.62, 148.59, 148.58, 133.68, 132.57, 131.04, 130.22, 130.21, 128.02, 127.42, 126.56, 124.34, 116.05, 115.89, 100.79, 95.06, 58.09, 32.65, 22.85, 22.34, 21,92. Anal. Calcd for $C_{24}H_{19}FN_4O_2$: C, 69.55; H, 4.62; N, 13.52. Found: C, 69.35; H, 4.33; N, 13.47.

5.3.10. *15-Amino-14-(o-tolyl)-2,3,4,14-tetrahydro-1H-quinolino[2',3':3,4]pyrazolo[1,2-b]phthalazine-7,12-dione (7j).* Yield 90%; off white solid; mp >250 ℃; IR (KBr, cm^{-1}) ν_{max}: 3481 and 3365 (NH$_2$), 1657 (C=O), 1600 (C=N). ^{1}H NMR (DMSO-d_6, 500 MHz) δ: 8.28 (dd, 1H, J = 6.5 Hz, H$_8$ phthalazine), 8.07 (dd, 1H, J = 7 Hz, H$_{11}$ phthalazine), 7.92 (m, 2H, H$_{9,10}$ phthalazine), 7.23 (d, 1H, J = 7 Hz, H$_3$ phenyl), 7.17 (m, 3H, H$_{4,5,6}$ phenyl), 6.74 (s, 1H, H$_{14}$), 5.05 (S, 2H, NH$_2$), 2.74 (bs, 2H, H$_2$ cyclohexyl), 2.43 (S, 3H, Me), 2.35-2.28 (m, 2H, cyclohexyl), 1.76 (bs, 4H, cyclohexyl). ^{13}C NMR (DMSO-d_6, 100 MHz) δ: 155.57, 153.60, 152.66, 148.52, 147.51, 136.29, 134.76, 133.56, 133.43, 130.76, 130.03, 128.24, 128.12, 127.29, 126.46, 114.11, 101.73, 59.94, 32.58, 22.72, 22.26, 21.83, 18.67. Anal. Calcd for $C_{25}H_{22}N_4O_2$: C, 73.15; H, 5.40; N, 13.65. Found: C, 72.97; H, 5.32; N, 13.55.

5.3.11. *15-Amino-14-(2-nitrophenyl)-2,3,4,14-tetrahydro-1H-quinolino[2',3':3,4]pyrazolo[1,2-b]phthalazine-7,12-dione (7k).* Yield 85%; off white solid; mp >250 ℃; IR (KBr, cm^{-1}) ν_{max}: 3483 and 3419 (NH$_2$), 1632 (C=O), 1522 (C=N). ^{1}H NMR (DMSO-d_6, 500 MHz) δ: 8.49 (m, 1H, H$_8$ phthalazine), 8.18 (m, 1H, H$_{11}$ phthalazine), 7.78 (m, 3H, H$_{9,10}$ phthalazine and H$_3$ phenyl), 7.42 (m, 3H, H$_{4,5,6}$ phenyl),

7.13 (s, 1H, H_{14}), 4.77 (S, 2H, NH_2), 2.98 (bs, 2H, cyclohexyl), 2.4 (bs, 2H, cyclohexyl), 1.86 (bs, 4H, cyclohexzyl). ^{13}C NMR (DMSO-d_6, 100 MHz) δ: 156.03, 153.57, 152.62, 149.90, 148.86, 134.07, 133.56, 133.51, 131.53, 130.31, 129.61, 128.75, 127.35, 126.36, 123.67, 116.05, 115.89, 100.79, 95.06, 56.31, 32.60, 22.74, 22.23, 21,78. Anal. Calcd for $C_{24}H_{19}N_5O_2$: C, 69.30; H, 4.34; N, 15.86. Found: C, 70.01; H, 4.83; N, 15.71.

5.3.12.   *15-Amino-14-(2-methoxyphenyl)-2,3,4,14-tetrahydro-1H-quinolino[2',3':3,4]pyrazolo[1,2-b]phthalazine-7,12-dione (7l).* Yield 75%; off white solid; mp >250 ºC; IR (KBr, cm^{-1}) ν_{max}: 3442 and 3350 (NH_2), 1668 (C=O), 1595 (C=N). ^1H NMR (DMSO-d_6, 500 MHz) δ: 8.32 (d, 1H, J = 7.5 Hz, H_8 phthalazine), 8.08 (d, 1H, J = 7.5 Hz, H_{11} phthalazine), 7.96 (m, 2H, $H_{9,10}$ phthalazin), 7.47 (d, 1H, H3 phenyl), 7.27 (td, 1H, J = 7 Hz, H_5 phenyl), 7.04 (d, 1H, J = 8.2 Hz, H_6 phenyl), 6.91 (t, 1H, J = 8 Hz, H_4 phenyl), 6.82 (s, 1H, H_{14}), 5.97 (S, 2H, NH_2), 3.72 (S, 3H, OMe), 2.76 (bs, 2H, cyclohexyl), 2.4-2.25 (m, 2H, cyclohexyl), 1.73 (bs, 4H, cyclohexyl). ^{13}C NMR (DMSO-d_6, 100 MHz) δ: 155. 97, 153.37, 134.12, 133.75, 131.44, 129.67, 128.62, 128.39, 127.46, 126.74, 124.55, 121.29, 114.13, 112.03, 101.87, 58.12, 56.07, 26.20, 22.70, 21.91, 21.60. Anal. Calcd for $C_{25}H_{22}N_4O_3$: C, 70.41; H, 5.20; N, 13.14. Found: C, 69.97; H, 4.62; N, 12.84.

5.3.13.   *15-Amino-14-(3,5-dimethoxyphenyl)-2,3,4,14-tetrahydro-1H-quinolino[2',3':3,4]pyrazolo[1,2-b]phthalazine-7,12-dione (7m).* Yield 85%; off white solid; mp >250 ºC; IR (KBr, cm^{-1}) ν_{max}: 3440 and 3420 (NH_2), 1633 (C=O), 1462 (C=N). ^1H NMR (DMSO-d_6, 500 MHz) δ: 8.29 (d, 1H, J = 7 Hz, H_8 phthalazine), 8.11 (d, 1H, J = 7 Hz, H_{11} phthalazine), 7.9 4 (m, 2H, $H_{9,10}$ phthalazin), 6.63 (m, 3H, $H_{2,4,6}$ phenyl), 6.41 (s, 1H, H_{14}), 5.71 (s, 2H, NH_2), 3.68 (s, 6H, 2OMe), 2.71 (bs, 2H, cyclohexyl), 2.42-2.27 (m, 2H, cyclohexyl), 1.75 (bs, 4H, cyclohexyl). ^{13}C NMR (DMSO-d_6, 100 MHz) δ: 160.34, 155. 42, 152.73, 147.72, 140.34, 133.46, 133.36, 130.10, 127.30, 126.47, 113.94, 105.64, 99.02, 95.36, 61.05, 55.07, 32.57, 22.73, 22.28, 21.87. Anal. Calcd for $C_{26}H_{24}N_4O_4$: C, 68.41; H, 5.30; N, 12.27. Found: C, 67.93; H, 5.21; N, 13.1.

5.3.14.   *15-Amino-14-(3-bromophenyl)-2,3,4,14-tetrahydro-1H-quinolino[2',3':3,4]pyrazolo[1,2-b]phthalazine-7,12-dione (7n).* Yield 90%; off white solid; mp >250 ºC; IR (KBr, cm^{-1}) ν_{max}: 3421 and 3354 (NH_2), 1637 (C=O), 1600 (C=N).

^{1}H NMR (DMSO-d_6, 500 MHz) δ: 8.28 (d, 1H, J = 7.5 Hz, H$_8$ phthalazine), 8.09 (d, 1H, J = 7.5 Hz, H$_{11}$ phthalazine), 7.93 (m, 2H, H$_{9,10}$ phthalazine), 7.82 (s, 1H, H$_2$ phenyl), 7.46 (d, 1H, J = 7 Hz, H$_4$ phenyl), 7.33 (d, 1H, J = 8 Hz, H$_6$ phenyl), 7.24 (d, 1H, J = 8 Hz, H$_5$ phenyl), 6.7 (S, 1H, H$_{14}$), 5.78 (S, 2H, NH$_2$), 2.73 (bs, 2H, cyclohexyl), 2.43-2.26 (m, 2H, cyclohexyl), 1.75 (bs, 4H, cyclohexyl). ^{13}C NMR (DMSO-d_6, 100 MHz) δ: 155.63, 153, 60, 148.39, 140.18, 133. 62, 130.97, 130.88, 130.69, 130.32, 128.21, 127.42, 126.57, 126.06, 121.36, 117.36, 113.91, 101.38, 95.50, 60.53, 32.68, 22.87, 22.35, 21.93. Anal. Calcd for C$_{24}$H$_{19}$BrN$_4$O$_2$: C, 60.64; H, 4.03; N, 11.79. Found: C, 61.38; H, 4.79; N, 10.11.

5.5.15 15-Amino-14-(3-fluorophenyl)-2,3,4,14-tetrahydro-1H-quinolino[2',3':3,4]pyrazolo[1,2-b]phthalazine-7,12-dione (7o). Yield 80%; off white solid; mp >250 ºC; IR (KBr, cm^{-1}) ν_{max}: 3485 and 3375 (NH$_2$), 1659 (C=O), 1587 (C=N). ^{1}H NMR (DMSO-d_6, 500 MHz) δ: 8.28 (d, 1H, J = 7.5 Hz, H$_8$ phthalazine), 8.09 (d, 1H, J = 7.5 Hz, H$_{11}$ phthalazine), 7.9 (m, 2H, H$_{9,10}$ phthalazine), 7.42 (d, 1H, J = 9.5 Hz, H$_4$ phenyl), 7.32 (q, 1H, J = 7 Hz, H$_2$ phenyl), 7.19 (d, 1H, J = 7 Hz, H$_6$ phenyl), 7.09 (t, 1H, J = 8 Hz, H$_5$ phenyl), 6.73 (s, 1H, H$_{14}$), 5.73 (s, 2H, NH$_2$), 2.73 (bs, 2H, cyclohexyl), 2.4-2.29 (m, 2H, cyclohexyl), 1.75 (bs, 4H, cyclohexyl). ^{13}C NMR (DMSO-d_6, 100 MHz) δ: 155.62, 152.91, 152.60, 148.09, 147.75, 145.54, 140.31, 133.51, 130.25, 130.26, 127.34, 126.50, 122.99, 114.98, 114.89, 102.9, 60.77, 32.61, 22.77, 22.29, 21.87. Anal. Calcd for C$_{24}$H$_{19}$FN$_4$O$_2$: C, 69.55; H, 4.62; N, 13.52. Found: C, 68.89; H, 4.68; N, 13.2.

5.5.16 15-Amino-14-(3-nitrophenyl)-2,3,4,14-tetrahydro-1H-quinolino[2',3':3,4]pyrazolo[1,2-b]phthalazine-7,12-dione (7p). Yield 80%; off white solid; mp >250 ºC; IR (KBr, cm^{-1}) ν_{max}: 3435 and 3358 (NH$_2$), 1633 (C=O), 1530 (C=N). ^{1}H NMR (DMSO-d_6, 500 MHz) δ: 8.54 (s, 1H, H$_2$ phenyl), 8.28 (d, 1H, J = 7.5 Hz, H$_8$ phthalazine), 8.13 (d, 1H, J = 8 Hz, H$_4$ phenyl), 8.08 (d, 1H, J = 7.5 Hz, H$_{11}$ phthalazine), 7.92 (m, 2H, H$_{9,10}$ phthalazine), 7.78 (d, 1H, J = 7.6 Hz, H$_6$ phenyl), 7.57 (t, 1H, J = 8 Hz, H$_5$ phenyl), 6.86 (S, 1H, H$_{14}$), 5.86 (S, 2H, NH$_2$), 2.73 (bs, 2H, cyclohexyl), 2.4-2.27 (m, 2H, cyclohexyl), 1.75 (bs, 4H, cyclohexyl). ^{13}C NMR (DMSO-d_6, 100 MHz) δ: 155.86, 153.77, 152.78, 148.57, 148.04, 147.44, 139.58, 133.86, 133.67, 130.42, 130.17, 128.19,

14

127.47, 126.60, 123.42, 123.23, 114.01, 101.06, 60.49, 32.74, 22.93, 22.39, 21.96. Anal. Calcd for $C_{24}H_{19}N_5O_4$: C, 65.30; H, 4.34; N, 15.86. Found: C, 64.56; H, 4.21; N, 15.08.

5.5.17.   15-Amino-14-(m-tolyl)-2,3,4,14-tetrahydro-1H-quinolino[2',3':3,4]pyrazolo[1,2-b]phthalazine-7,12-dione (7q). Yield 95%; off white solid; mp >250 ºC; IR (KBr, cm^{-1}) ν_{max}: 3482 and 3350 (NH$_2$), 1678 (C=O), 1600 (C=N). ^{1}H NMR (DMSO-d_6, 500 MHz) δ: 8.28 (d, 1H, J = 7.5 Hz, H$_8$ phthalazine), 8.08 (d, 1H, J = 7.5 Hz, H$_{11}$ phthalazine), 7.93 (m, 2H, H$_{9,10}$ phthalazine), 7.25 (m, 2H, H$_{2,4}$ phenyl), 7.18 (t, 1H, J = 7.5 Hz, H$_5$ phenyl), 7.06 (d, 1H, J = 7.5 Hz, H$_6$ phenyl), 6.67 (S, 1H, H$_{14}$), 5.66 (s, 2H, NH$_2$), 2.72 (bs, 2H, cyclohexyl), 2.4-2.27 (m, 2H, cyclohexyl), 2.23 (s, 3H, 3-Me), 1.75 (bs, 4H, cyclohexyl). ^{13}C NMR (DMSO-d_6, 100 MHz) δ: 155.35, 152.75, 147.77, 137.48, 133.63, 133.49, 130.21, 128.77, 128.36, 128.24, 127.80, 127.40, 126.56, 124.56, 113.86, 102.16, 61.20, 32.66, 22.87, 22.38, 21.95, 20.99. Anal. Calcd for $C_{25}H_{22}N_4O_2$: C, 73.15; H, 5.40; N, 13.65. Found: C, 73.22; H, 5.03; N, 12.99.

5.5.18.   15-Amino-14-(3-hydroxyphenyl)-2,3,4,14-tetrahydro-1H-quinolino[2',3':3,4]pyrazolo[1,2-b]phthalazine-7,12-dione (7r). Yield 75%; off white solid; mp >250 ºC; IR (KBr, cm^{-1}) ν_{max}: 3481 and 3449 (NH$_2$), 1641 (C=O), 1577 (C=N). ^{1}H NMR (DMSO-d_6, 500 MHz) δ: 9.38 (s, 1H, OH), 8.28 (d, 1H, J = 7.5 Hz, H$_8$ phthalazine), 8.09 (d, 1H, J = 7.5 Hz, H$_{11}$ phthalazine), 7.93 (m, 2H, H$_{9,10}$ phthalazine), 7.08 (t, 1H, J = 7.9 Hz, H$_5$ phenyl), 6.92 (d, 1H, J = 7.7 Hz, H$_6$ phenyl), 6.76 (bs, H$_2$ phenyl), 6.66 (S, 1H, H$_{14}$), 6.64 (d, 1H, J = 8 Hz, H$_4$ phenyl), 5.72 (S, 2H, NH$_2$), 2.72 (bs, 2H, cyclohezyl), 2.42-2.26 (m, 2H, cyclohexyl), 1.75 (bs, 4H, cyclohexyl). ^{13}C NMR (DMSO-d_6, 100 MHz) δ: 157.33, 155.60, 153.55, 148.28, 139.05, 133.66, 133.49, 129.24, 128.35, 127.37, 126.57, 118.28, 117.07, 115.16, 113.87, 102.07, 61.04, 32.63, 22.81, 22.34, 21.93. Anal. Calcd for $C_{24}H_{20}N_4O_3$: C, 69.89; H, 4.89; N, 13.58. Found: C, 70.11; H, 5.06; N, 13.83.

5.3.19.   15-Amino-14-methyl-2,3,4,14-tetrahydro-1H-quinolino[2',3':3,4]pyrazolo[1,2-b]phthalazine-7,12-dione (7s). Yield 70%; off white solid; mp >250 ºC; IR (KBr, cm^{-1}) ν_{max}: 3480 and 3349 (NH$_2$), 1641 (C=O), 1588 (C=N). ^{1}H NMR (DMSO-d_6, 500 MHz) δ: 8.23 (d, 2H, J = 2 Hz, H$_{8,11}$ phthalazine), 7.94 (bs, 2H, H$_{9,10}$ phthalazine), 6.14 (s, 2H, NH$_2$), 5.79 (S, 1H, H$_{14}$), 2.67 (bs, 2H, cyclohexyl), 2.4-2.1 (m, 2H, cyclohexyl), 1.75 (bs, 4H,

cyclohexyl), 1.55 (d, 3H, , $J = 6$ Hz, CH$_3$). ^{13}C NMR (DMSO-d_6, 100 MHz) δ: 154.95, 153.75, 152.77, 149.48, 133.63, 133.40, 130.21, 128.77, 127.32, 126.53, 113.86, 100.16, 55.23, 32.68, 23.01, 22.49, 22.12, 16.54. Anal. Calcd for C$_{19}$H$_{18}$N$_4$O$_2$: C, 68.25; H, 5.43; N, 16.76. Found: C, 68.71; H, 5.10; N, 16.62.

5.3.20. *15-Amino-14-propyl-2,3,4,14-tetrahydro-1H-quinolino[2',3':3,4]pyrazolo[1,2-b]phthalazine-7,12-dione (7t).* Yield 70%; off white solid; mp >250 ºC; IR (KBr, cm^{-1}) ν_{max}: 3478 and 3415 (NH$_2$), 2980 (CH aliphatic), 1661 (C=O), 1567 (C=N). ^{1}H NMR (DMSO-d_6, 500 MHz) δ: 8.24 (d, 2H, $J = 2$ Hz, H$_{8,11}$ phthalazine), 7.95 (bs, 2H, H$_{9,10}$ phthalazine), 6.09 (s, 2H, NH$_2$), 5.93 (s, 1H, H$_{14}$), 2.69 (bs, 2H, cyclohexyl), 2.43-2.31 (m, 2H, cyclohexyl), 1.99 (t, 2H, CH$_2$), 1.76 (bs, 4H, cyclohexyl), 0.94-0.85 (m, 2H, CH$_2$), 0.71 (t, 3H, , $J = 6.9$ Hz, CH$_3$). ^{13}C NMR (DMSO-d_6, 100 MHz) δ: 154.94, 153.85, 152.64, 149.02, 147.99, 133.69, 133.46, 130.09, 128.31, 127.34, 126.63, 113.52, 99.85, 58.95, 32.68, 30.23, 22.98, 22.48, 22.11, 15.71, 13.80. Anal. Calcd for C$_{21}$H$_{22}$N$_4$O$_2$: C, 69.59; H, 6.12; N, 15.46. Found: C, 68.03; H, 5.50; N, 16.58.

5.3.21. *15-Amino-14-pentyl-2,3,4,14-tetrahydro-1H-quinolino[2',3':3,4]pyrazolo[1,2-b]phthalazine-7,12-dione (7u).* Yield 75%; off white solid; mp >250 ºC; IR (KBr, cm^{-1}) ν_{max}: 3478 and 3374 (NH$_2$), 2980 (CH aliphatic), 1656 (C=O), 1563 (C=N). ^{1}H NMR (DMSO-d_6, 500 MHz) δ: 8.24 (m, 2H, H$_{8,11}$ phthalazine), 7.95 (m, 2H, H$_{9,10}$ phthalazine), 6.08 (s, 2H, NH$_2$), 5.93 (s, 1H, H$_{14}$), 2.69 (bs, 2H, 2H$_9$), 2.43-2.31 (m, 4H, cyclohexyl), 2.02 (m, 2H, CH$_2$), 1.77 (bs, 4H, cyclohexyl), 1.08 (m, 2H, CH$_2$), 0.94-0.8 (m, 2H, CH$_2$), 0.68 (t, 3H, $J = 6.6$ Hz, CH$_3$). ^{13}C NMR (DMSO-d_6, 100 MHz) δ: 154.87, 153.81, 152.58, 148.97, 147.94, 133.63, 133.39, 130.02, 128.25, 127.29, 126.57, 113.45, 99.75, 58.93, 32.62, 30.99, 27.72, 22.91, 22.42, 22.05, 21.74, 13.71. Anal. Calcd for C$_{23}$H$_{26}$N$_4$O$_2$: C, 70.75; H, 6.71; N, 14.35. Found: C, 70.74; H, 6.51; N, 14.12.

5.4. In vitro AChE/BuChE inhibition assay

The anti-cholinesterase activity of target compounds **7a-u** was assessed in vitro against AChE from *Electrophorus electricus* (*eel*AChE) and horse serum butyrylcholinesterase (*eq*BuChE) by using the spectrophotometric method of Ellman [32]. In order to obtain a

range of 20-80% enzyme inhibition, five different concentrations of each compound were tested. A mixture of phosphate buffer (0.1 mol/L^{-1}, pH 8.0, 3 mL), 5,5′-dithio-bis(2-nitrobenzoic acid) (DTNB, 100 μL), acetylcholinesterase or butyrylcholinesterase (100 μL, 2.5 IU/mL) and compound solution (100 µL) was pre-incubated for 10 min. Then, the substrate (acetylthiocholine iodide or butyrylthiocholine iodide) was added. In parallel, a blank containing all components without enzyme was used in order to account the non-enzymatic reaction. Changes in absorbance were measured at 412 nm for 6 min at 25 °C by using an UV Unico Double Beam spectrophotometer. The IC$_{50}$ values were determined graphically from log concentration vs. % of inhibition curves. All experiments were performed in triplicate.

5.5. Determination of the inhibitory potency on Aβ$_{1-42}$ self-aggregation

In order to investigate the Aβ$_{1-42}$ self-aggregation, a ThT-based fluorometric assay was performed [33, 34]. 1,1,1,3,3,3-hexafluoro-2-propanol (HFIP) pre-treated Aβ sample (Bachem company, Switzerland) was diluted in assay buffer to have a stock solution ([Aβ 1-42]= 50 mM). Experiments were performed by incubating the peptide in phosphate buffer (pH 7.4), at 37 °C for 48 h (final Aβ concentration = 25 mM, 10 mL) with and without inhibitor. The inhibitor was dissolved in DMSO and diluted in the assay buffer at a final concentration of 10 µM. Blanks containing inhibitor and ThT were also prepared and evaluated to account for quenching and fluorescence properties. After incubation, samples were diluted to a final volume of 200 mL with 180 mL ThT (5 mM in 50 mM glycine-NaOH buffer, pH 8.5). The fluorescence intensity was carried out with multi-mode plate reader (EnSpire, PerkinElmer Waltham, Massachusetts, United States) at (λ_{ex} = 446 nm; λ_{em} = 490 nm), each assay was run in triplicate and each reaction was repeated at least three independent times, values at plateau were averaged after subtracting the background fluorescence of 5 mM ThT solution. The fluorescence intensities were compared and the % inhibition was calculated by the following equation: $100 - [(IF_i - IF_b)/(IF_o - IF_b) \times 100]$ where IF_i, IF_o and IF_b are the fluorescence intensities obtained for Aβ aggregation in the presence of inhibitors, in the absence of inhibitors and the blanks, respectively.

5.6. Determination of the inhibitory potency on Aβ$_{1-40}$ aggregation induced by AchE

For co-incubation experiments [35, 36] of Aβ (1-40) trifluoroacetate salt (Bachem company, Switzerland) and AChE from (Sigma, *Electrophorus electricus*), the mixtures of Aβ$_{1-40}$ peptide and AChE in presence or absence of the test inhibitor were incubated for 24 h at room temperature. The final concentrations of Aβ (dissolved in DMSO and diluted 0.215 M sodium phosphate buffer, pH 8), AChE (dissolved in 0.215 M sodium phosphate buffer, pH 8.0) and the tested compound are 200 µM, 2 µM and 100 µM respectively. To analyze co-aggregation inhibition, the ThT fluorescence method was used and the fluorescence was measured with multi-mode plate reader (EnSpire, PerkinElmer Waltham, Massachusetts, United States) at (λ_{ex} = 446 nm; λ_{em} = 490 nm). After co-incubation, 20 µL of the mixture solutions was diluted to a final volume of 2 mL with ThT (1.5 µM in 50 mM glycine-NaOH buffer, pH 8.5). Blanks containing Aβ, AChE, Aβ plus the tested compound, and AChE plus the tested compound in 0.215 M sodium phosphate buffer (pH 8.0) were prepared. The percent inhibition of the AChE-induced aggregation due to the presence of inhibitor was calculated by the following expression: $100 - [(IF_i - IF_b)/(IF_o - IF_b) \times 100]$ where IF_i, IF_o and IF_b are the fluorescence intensities obtained for Aβ aggregation in the presence of inhibitors, in the absence of inhibitors and the blanks, respectively. Each assay was run in triplicate and each reaction was repeated at least three independent times.

5.7. Neuroprotection assay against H$_2$O$_2$-induced cell death in PC12 cells

The neuroprotection assay was conducted by using rat differentiated PC12 cells [37]. The differentiated PC12 cells were treated with different concentrations (1, 10, 50 and 100 µM) of the compound and incubated for 3 h before treatment with H_2O_2 (350 µM). The DAPI staining was used for checking the occurrence of apoptosis. The cell viability was measured after 24 h by using the MTT assay. Briefly, MTT solution (10 µL, 5 mg/mL, Sigma) was added to the cultured PC12 cells (150 µL) and incubated in a CO_2 incubator for 3.5 h. Thereafter, medium was removed and DMSO (150 µl) was added into the each well for dissolving the precipitated formazan. The dye dissolution was facilitated by shaking the plate for 10 min at speed of 120 rpm. Finally, optical density (OD) was determined at 560 nm on the microplate reader (BioTek synergy HT). Results were adjusted considering OD measured in the blank [38].

18

5.8. In vitro cytotoxicity assay against HepG2 cells

In order to investigate the effect of selected compounds **7b-d** and **7o** on cell viability, the MTT assay was performed using HepG2 cell line. The cell line was provided from Iranian Biological Resource Center (IBRC, Tehran, Iran) and subcultured in DMEM medium containing FBS (10%) at 37 °C under 5% CO_2 in a humidified chamber. The cell was harvested in exponential phase of growth and seeded into 96-well tissue culture microplate (1.5×10^4 cells/well) and incubated at 37 °C for 24 h to adhere. The medium was then removed and cells were exposed (for further 24 h) to desired concentrations (1–300 µM) of each compound which previously dissolved in FBS-free DMEM medium. Thereafter, the medium of each well was replaced by MTT solution (5 mg/mL) and incubated for 4 h to form formazan crystal which was then dissolved by addition of DMSO (100 µL). The related absorbance (540 nm) was consequently recorded using a Synergy 2 multi-mode plate reader apparatus (Biotek, Winooski, VT, USA) and applied to determine the viability percent regarding to that of the control. Three independent replicates of each experiment were performed and mean of the obtained results was reported.

5.9. Docking simulations

The program Autodock Vina was used for docking simulations [39]. The crystal structure of *Torpedo californica* acetylcholinesterase (1EVE) was retrieved from Protein Data Bank (http://www.rcsb.org/pdb/home/home.do). To create receptor and ligand structures for docking, the following procedure was conducted. First, the co-crystallized ligand and water molecules were removed from the protein. After that the atomic coordinates of the ligands was prepared using Marvinsketch, 2012, ChemAxon (http://www.chemaxon.com), the 3D structures were constructed using Openable [40]. Then, the receptor and optimized structure of the ligands were converted to required pdbqt format using Autodock Tools [41]. The Autodock Vina parameters were set as follow; box size: $15 \times 15 \times 15$ Å, the center of box: x = 2.023, y = 63.295, z = 67.062 (geometrical center of co-crystallized ligand), the exhaustiveness: 100, and the remaining parameters were left unchanged. The calculated geometries were ranked in terms of free energy of binding and the best poses were selected

for further analysis. All molecular visualizations were carried out in DS Viewer Pro (Accelrys, Inc., San Diego, CA).

Acknowledgments

References

[1] M. Prince, A. Wimo, M. Guerchet, G-C. Ali, Y-T. Wu, M. Prina, World Alzheimer Report 2015, A. D. I. London (2015).

[2] C.L. Masters, R. Bateman, K. Blennow, C.C. Rowe, R.A. Sperling, J.L. Cummings, Alzheimer's disease, Nat. Rev. Dis. Primers 1 (2015) 15056.

[3] R. León, AG. Garcia, J. Marco-Contelles. Recent advances in the multitarget-directed ligands approach for the treatment of Alzheimer's disease, Med. Res. Rev. 33 (2013) 139-189.

[4] J. Hroudová, N. Singh, Z. Fišar, K. K. Ghosh, Progress in drug development for Alzheimer's disease: An overview in relation to mitochondrial energy metabolism, Eur. J. Med. Chem. 121 (2016) 774-784.

[5] M. Wu, G. Esteban, S. Brogi, M. Shionoya, L. Wang, G. Campiani, M. Unzeta, T. Inokuchi, S. Butini, J. Marco-Contelles, Donepezil-like multifunctional agents: Design, synthesis, molecular modeling and biological evaluation, Eur. J. Med. Chem. 121 (2016) 864–879.

[6] E. Giacobini, Cholinesterase inhibitors: new roles and therapeutic alternatives, Pharmacol. Res. 50 (2004) 433–440.

[7] G.T. Grossberg, Cholinesterase inhibitors for the treatment of Alzheimer's disease: Getting on and staying on, Curr. Ther. Res. Clin. Exp. 64 (2003) 216–235.

[8] N.C. Inestrosa, A. Alvarez, C.A. Pérez, R.D. Moreno, M. Vicente, C. Linker, O.I. Casanueva, C. Soto, J. Garrido, Acetylcholinesterase accelerates assembly of amyloid-beta-peptides into Alzheimer's fibrils: possible role of the peripheral site of the enzyme, Neuron, 16 (1996) 881–891.

[9] D. Praticò, Oxidative stress hypothesis in Alzheimer's disease: a reappraisal, Trends Pharmacol. Sci. 29 (2008) 609–615.

[10] P.C. Trippier, K. Jansen Labby, D.D. Hawker, J.J. Mataka, R.B. Silverman, Target- and mechanism-based therapeutics for neurodegenerative diseases: strength in numbers, J. Med. Chem. (2013) 3121–3147.

[11] F.M. Longo, S.M. Massa, Neuroprotective strategies in Alzheimer's disease, Neuron Rx. 1 (2004) 117–127.

[12] G.W. Small, Tacrine for treating Alzheimer's disease, JAMA 268 (1992) 2564–2565.

[13] M.L. Crismon, Tacrine: first drug approved for Alzheimer's disease, Ann. Pharmacother. 28 (1994) 744-751.

[14] P.B. Watkins, H.J. Zimmerman, M.J. Knapp, S.I. Gracon, K.W. Lewis, Hepatotoxic effects of tacrine administration in patients with Alzheimer's disease, JAMA 271 (1994) 992–998.

[15] E. Nepovimova, J. Korabecny, R. Dolezal, K. Babkova, A. Ondrejicek, D. Jun, V. Sepsova, A. Horova, M. Hrabinova, O. Soukup, N. Bukum, P. Jost, L. Muckova, J. Kassa, D. Malinak, M. Andrs, K. Kuca, Tacrine-trolox hybrids: a novel class of centrally active, nonhepatotoxic multi-target-directed ligands exerting anticholinesterase and antioxidant activities with low in vivo toxicity, J. Med. Chem. 58 (2015) 8985–9003.

[16] M. del Monte-Millán, E. García-Palomero, R. Valenzuela, P. Usán, C. de Austria, P. Muñoz- Ruiz, L. Rubio, I. Dorronsoro, A. Martínez, M. Medina, Dual binding site acetylcholinesterase inhibitors: potential new disease-modifying agents for AD, J. Mol. Neurosci. 30 (2006) 85–88.

[17] A. Romero, R. Cacabelos, M. J. Oset-Gasque, A. Samadi, J. Marco-Contelles, Novel tacrine-related drugs as potential candidates for the treatment of Alzheimer's disease, Bioorg. Med. Chem. Lett. 23 (2013) 1916–1922.

[18] M. Khoobi, F. Ghanoni, H. Nadri, A. Moradi, M. Pirali Hamedani, F. Homayouni Moghadam, S. Emami, M. Vosooghi, R. Zadmard, A. Foroumadi, A. Shafiee, New tetracyclic tacrine analogs containing pyrano[2,3-c]pyrazole: efficient synthesis, biological assessment and docking simulation study, Eur. J. Med. Chem. 89 (2015) 296–303.

[19] L. Pourabdi, M. Khoobi, H. Nadri, A. Moradi, F.H. Moghadam, S. Emami, M.M. Mojtahedi, I. Haririan, H. Forootanfar, A. Ameri, A. Foroumadi, A. Shafiee, Synthesis

and structure-activity relationship study of tacrine-based pyrano[2,3-c]pyrazoles targeting AChE/BuChE and 15-LOX, Eur. J. Med. Chem. 123 (2016) 298–308.

[20] E.J. Barreiro, C.A. Camara, H. Verli, L. Brazil-Más, N.G. Castro, W.M. Cintra, Y. Aracava, C.R. Rodrigues, C.A. Fraga, Design, synthesis, and pharmacological profile of novel fused pyrazolo[4,3-d]pyridine and pyrazolo[3,4-b][1,8]naphthyridine isosteres: a new class of potent and selective acetylcholinesterase inhibitors, J. Med. Chem. 46 (2003) 1144–1152.

[21] C. Yamalı, M. Ozan Gülcan, B. Katya, S. kübanoĝlu, M.K. Süküroĝlu, D.S. Doĝruer, Synthesis of some 3(2H)-pyridazinone and 1(2H)-phthalazinone derivatives incorporating aminothiazole moiety and investigation of their antioxidant, acetylcholinesterase, and butyrylcholinesterase inhibitory activities, J. Med. Chem. Res. 24 (2015) 1210–1217.

[22] B. Kılıç, H.O. Gülcan, M. Yalçın, F. Aksakal, A. Dimoglo, M.F. Şahin, D.S. Doĝruer, Synthesis of some new 1(2H)-phthalazinone derivatives and evaluation of their acetylcholinesterase and butyrylcholinesterase inhibitory activities, Lett. Drug Des. Discov. 13 (E-pub ahead of print).

[23] D. Silva, M. Chioua, A. Samadi, M. C. Carreiras, M-L. Jimeno, E. Mendes, Cde. L. Ríos, A. Romero, M. Villarroy, M. G. LÓpez, J. Marco-Contelles, Synthesis and pharmacological assessment of diversely substituted pyrazolo[3,4-b]quinoline, and benzo[b]pyrazolo[4,3-g][1,8]naphthyridine derivatives, Eur. J. Med. Chem. 46 (2011) 4676–4681.

[24] D. Silva, M. Chioua, A. Samadi, P. Agostinho, P. Garção, R. Lajarín-Cuesta, Cde. L. Ríos, I. Iriepa, I. Moraleda, L. Gonzalez-Lafuente, E. Mendes, C. Pérez, M. I. Rodríguez-Franco, J. Marco-Contellese, M. C. Carreiras, Synthesis, pharmacological assessment, and molecular modeling of acetylcholinesterase/butyrylcholinesterase inhibitors: Effect against amyloid-β-induced neurotoxicity, ACS Chem. Neurosci. 4 (2013) 547–565.

[25] S.H. Song, J. Zhong, Y.H. He, Z. Guan, One-pot four-component synthesis of 1H-pyrazolo[1,2-b]phthalazine-5,10-dione derivatives, Tetrahedron Lett. 53 (2012) 7075–7077.

[26] J. Marco-Contelles, E. Pérez-Mayoral, A. Samadi, M. do C. Carreiras, E, Soriano, Recent Advances in the Friedländer Reaction, Chem. Re. 109 (2009) 2652–2671.

[27] D. Lagadic-Gossmann, M. Rissel, M. A. Le Bot, A. Guillouzo, Toxic effects of tacrine on primary hepatocytes and liver epithelial cells in culture. Cell Biol. Toxicol, 14 (1998) 361–373.

[28] M.W. Fariss, V.R. Mumaw, L.P. Walton, Tetrahydroaminoacridine-induced apoptosis in rat hepatocytes, Toxicol. In Vitro. 10 (1996) 383–393.

[29] M. Pohanka, Alzheimer´s disease and oxidative stress: a review, Curr. Med. Chem. 21 (2014) 356–364.

[30] F. Cheng, W. Li, Y. Zhou, J. Shen, Z. Wu, G. Liu, P. W. Lee, Y. Tang, admet SAR: a comprehensive source and free tool for evaluating chemical ADMET properties. J. Chem. Inf. Model. 52 (2012) 3099–3105.

[31] M. Khoobi, M. Alipour, A. Moradi, A. Sakhteman, H. Nadri, S.F. Razavi, M. Ghandi, A.Foroumadi, A. Shafiee, Design, synthesis, docking study and biological evaluation of some novel tetrahydrochromeno [3',4':5,6]pyrano[2,3-b]quinolin-6(7H)-one derivatives against acetyl- and butyrylcholinesterase, Eur. J. Med. Chem. 68 (2013) 291–300.

[32] G.L. Ellman, K.D. Courtney, V. Andres, R.M. Featherstone, A new and rapid colorimetric determination of acetylcholinesterase activity. Biochem. Pharmacol. 7 (1961) 88–95.

[33] M. Bartolini, C. Bertucci, M. L. Bolognesi, A. Cavalli, C. Melchiorre, V. Andrisano, Insight into the kinetic of amyloid beta (1-42) eptide self-aggregation: elucidation of inhibitors' mechanism of action, Chembiochem. 8 (2007) 2152–2161.

[34] G-F. Zha, C-P. Zhang, H-L. Qin, I. Jantan, M. Sher, M.W. Amjad, M.A. Hussain, Z. Hussain, S.N.A. Bukhari, Biological evaluation of synthetic α,β unsaturated carbonyl based cyclohexanone derivatives as neuroprotective novel inhibitors of acetylcholinesterase, butyrylcholinesterase and amyloid-β aggregation, Bioorg. Med. Chem. 24 (2016) 2352–2359.

[35] M. Bartolini, C. Bertucci, V. Cavrini, V. Andrisano, β-amiloid aggregation induced by human acetylcholinesterase: inhibition studies, Biochem. Pharmacol. 65 (2003) 407–416.

[36] J. Rouleau, B.I. Iorga, C. Guillou, New potent human acetylcholinesterase inhibitors in the tetracyclic triterpene series with inhibitory potency on amyloid β aggregation, Eur. J. Med. Chem. 46 (2011) 2193–2205.

[37] S.H. Koh, S.H. Kim, H. Kwon, Y. Park, K.S. Kim, C.W. Song, J. Kim, M.H. Kim, H.J. Yu, J.S. Henkel, H.K. Jung, Epigallocatechin gallate protects nerve growth factor differentiated PC12 cells from oxidative-radical-stress-induced apoptosis through its effect on phosphoinositide 3-kinase/Akt and glycogen synthase kinase-3, Brain Res. Mol. Brain Res. 118 (2003) 72–81.

[38] D. Zsolt, A. Juhász, M. Gálfi, K. Soós, R. Papp, D. Zádori, B. Penke, Method for measuring neurotoxicity of aggregating polypeptides with the MTT assay on differentiated neuroblastoma cells, Brain Res. Bull. 62 (2003) 223–229.

[39] O. Trott, A.J. Olson, AutoDock Vina: improving the speed and accuracy of docking with a new scoring function, efficient optimization, and multithreading, J. Comput. Chem. 31 (2010) 455–461.

[40] N.M. O'Boyle, M. Banck, C.A. James, C. Morley, T. Vandermeersch, G.R. Hutchison, Open Babel: An open chemical toolbox, J. Cheminform, 3 (2011) 33.

[41] M.F. Sanner, A programming language for software integration and development, J. Mol. Graph. Model. 17 (1999) 57–61.

Captions:

Figure 1. The structures of tacrine, previously reported pyrazolo-quinoline analog of tacrine and newly designed tacrine-like compounds **7a-u** bearing an annulated pyrazolo[1,2-*b*]phthalazine nucleus.

Figure 2. *Left*: Lineweavere-Burk plot for the inhibition of AChE by compound **7l** at different concentrations of substrate (ATCh), *Right:* Secondary plot for calculation of steady-state inhibition constant (K_i) of compound **7l**.

Figure 3. Neuroprotective effect of compound **7l** against H_2O_2-induced cell death in PC12 cells. Data are expressed as Mean ± SD ($n = 8$), ****: P<0.0001, ***: P<0.001, *: P<0.01 all vs. control group.

Figure 4. The proposed orientation of compound **7l** in the AChE active site.

Figure 5. The binding mode of compound **7l** in the active site of AChE.

Scheme 1. Synthesis of compounds **7a-u**.

Table 1

Inhibitory activity of the target compounds **7a-u** against AChE and BuChE.
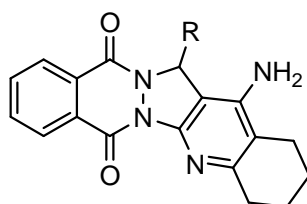
Compound	R	IC$_{50}$ (μM)[a] AChE	IC$_{50}$ (μM) BuChE
7a	Phenyl	0.614	>100
7b	4- Chlorophenyl	0.060	96.2
7c	4- Bromophenyl	0.080	>100
7d	4- Fluorophenyl	0.069	>100
7e	*p*-Tolyl	0.100	>100
7f	4- Nitrophenyl	0.310	>100
7g	2- Chlorophenyl	0.592	>100
7h	2-Bromophenyl	0.599	>100
7i	2- Fluorophenyl	0.618	>100
7j	*o*-Tolyl	0.193	>100
7k	2-Nitrophenyl	0.280	>100
7l	2-Methoxyphenyl	0.049	93.28
7m	3,5-Dimethoxyphenyl	3.37	>100
7n	3-Bromophenyl	0.271	>100
7o	3-Fluorophenyl	0.023	37.2
7p	3-Nitrophenyl	0.140	>100
7q	*m*-Tolyl	0.467	>100
7r	3-Hydroxophenyl	0.160	>100
7s	Methyl	2.15	>100
7t	Propyl	1.63	>100
7u	Pentyl	0.612	>100
Tacrine	-	0.365	0.013

[a]Data are expressed as mean ± S.E. of at least three different experiments.

Table 2
Inhibition of AChE-induced and self-induced Aβ aggregation by compound **7l** in comparison with tacrine and donepezil.

Compound	Inhibition of Aβ aggregation (%)	
	Self-induced[a]	AChE-induced[b]
7l	25.5 ± 2.9	32.0 ± 4.0
Tacrine	NT[c]	7.0 ± 0.5
Donepezil	15.4 ± 4.2	25.0 ± 2.0

[a] Inhibition of self-induced Aβ(1-42) aggregation (25 mM) produced by the tested compound at 10 µM concentration. Values are expressed as means ± SEM of three experiments.
[b] Co-aggregation inhibition of Aβ(1-40) and AChE (2 µM, ratio 100:1) by the tested compound at 100 µM concentration was detected by ThT assay. Values are expressed as means ± SEM of three experiments.
[c] Not tested.

Table 3

The effect of selected compounds **7b-d**, **7l and 7o** on the viability of HepG2 cell line at different concentrations.

Compound	Viability (%) of HepG2 cells						
	1 µM	5 µM	10 µM	25 µM	50 µM	100 µM	300 µM
7b	98.6 ± 1.3^{ns}	96.2 ± 0.9^{ns}	95.1 ± 2.2^{ns}	$94.4\pm1.1^{*}$	$92.4\pm1.1^{*}$	$91.3\pm1.2^{*}$	$89.3\pm0.4^{*}$
7c	99.8 ± 1.2^{ns}	98.3 ± 0.5^{ns}	97.6 ± 1.2^{ns}	96.4 ± 1.4^{ns}	95.7 ± 2.2^{ns}	$92.8\pm1.5^{*}$	$90.0\pm1.3^{*}$
7d	$91.2\pm1.6^{*}$	$87.5\pm1.3^{**}$	$83.3\pm1.3^{**}$	$80.0\pm0.7^{**}$	$75.9\pm2.2^{**}$	$71.4\pm1.4^{**}$	$66.4\pm2.1^{**}$
7o	$93.5\pm1.7^{*}$	$90.9\pm1.2^{*}$	$86.1\pm2.1^{**}$	$82.7\pm1.6^{**}$	$78.8\pm1.4^{**}$	$74.8\pm2.1^{**}$	$68.2\pm1.4^{**}$
7l	96.3 ± 0.8^{ns}	95.0 ± 1.6^{ns}	95.2 ± 0.5^{ns}	$90.2\pm1.1^{*}$	$87.3\pm0.2^{*}$	$86.4\pm1.4^{**}$	$83.0\pm0.7^{**}$
Tacrine	$94.2\pm1.3^{*}$	$90.3\pm0.9^{**}$	$77.3\pm1.1^{**}$	$73.3\pm0.7^{**}$	$66.4\pm1.2^{**}$	$58.3\pm2.2^{**}$	$43.2\pm0.9^{**}$

Cell viability was determined using MTT assay protocol. Data are expressed as the mean ± SEM of three independent replicates. The significant (**$p \leq 0.01$, *$p \leq 0.05$) and not significant (ns) values with respect to control group were obtained after one-way ANOVA analysis followed by Newman-Keuls post hoc test.

Table 4

The ADMET properties of compound **7a-u** predicted using admetSAR web-based application.

Compounds	BBB[a]	HIA[b]	Caco-2[c]	Carcinogens
7a	0.9900	1.0000	0.5167	Non Carcinogens
7b	0.9821	1.0000	0.6198	Non Carcinogens
7c	0.9805	1.0000	0.6086	Non Carcinogens
7d	0.9856	1.0000	0.6311	Non Carcinogens
7e	0.9843	1.0000	0.5000	Non Carcinogens
7f	0.9424	0.9952	0.5812	Non Carcinogens
7g	0.9673	1.0000	0.6311	Non Carcinogens
7h	0.9637	1.0000	0.6175	Non Carcinogens
7i	0.9734	1.0000	0.6423	Non Carcinogens
7j	0.9695	1.0000	0.5000	Non Carcinogens
7k	0.9080	0.9959	0.5809	Non Carcinogens
7l	0.9260	1.0000	0.5211	Non Carcinogens
7m	0.9112	1.0000	0.5540	Non Carcinogens
7n	0.9805	1.0000	0.6086	Non Carcinogens
7o	0.9856	1.0000	0.6311	Non Carcinogens
7p	0.9424	0.9952	0.5812	Non Carcinogens
7q	0.9843	1.0000	0.5000	Non Carcinogens
7r	0.8615	1.0000	0.6502	Non Carcinogens
7s	0.9835	1.0000	0.5055	Non Carcinogens
7t	0.9791	1.0000	0.5561	Non Carcinogens
7u	0.9807	1.0000	0.5687	Non Carcinogens

[a] Probablity of Blood Brain Barrier penetration
[b] Probablity of Human Intestinal Absorption
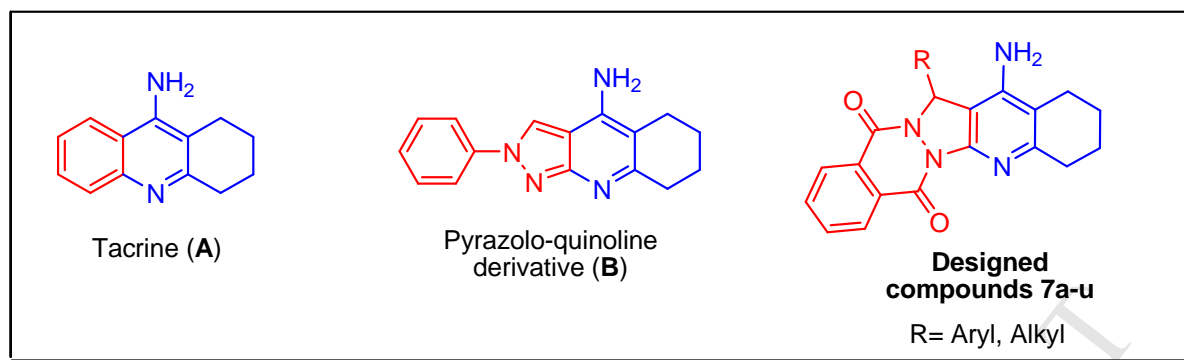[c] Probablity of Caco-2 permeation

Figure 1. The structures of tacrine, previously reported pyrazolo-quinoline analog of tacrine and newly designed tacrine-like compounds **7a-u** bearing an annulated pyrazolo[1,2-*b*]phthalazine nucleus.
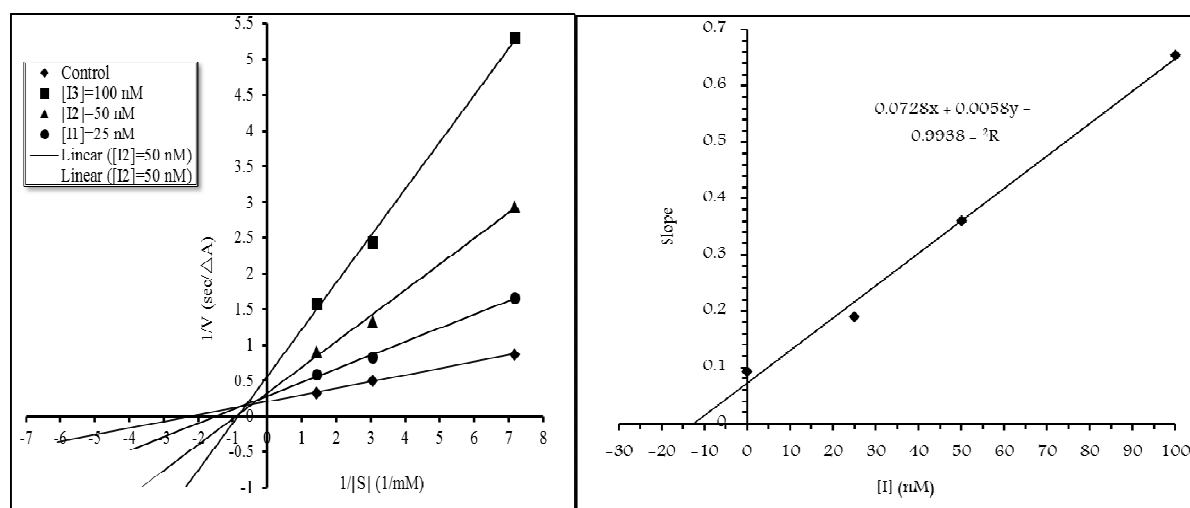
30

Figure 2. *Left*: Lineweavere-Burk plot for the inhibition of AChE by compound **7l** at different concentrations of substrate (ATCh), *Right:* Secondary plot for calculation of steady-state inhibition constant (K_i) of compound **7l**.
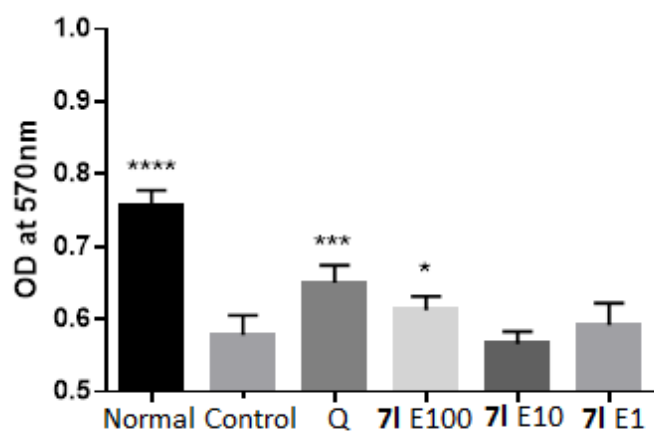
Figure 3. Neuroprotective effect of compound **7l** against H_2O_2-induced cell death in PC12 cells. Data are expressed as Mean ± SD (n = 8), ****: P<0.0001, ***: P<0.001, *: P<0.01 all vs. control group.
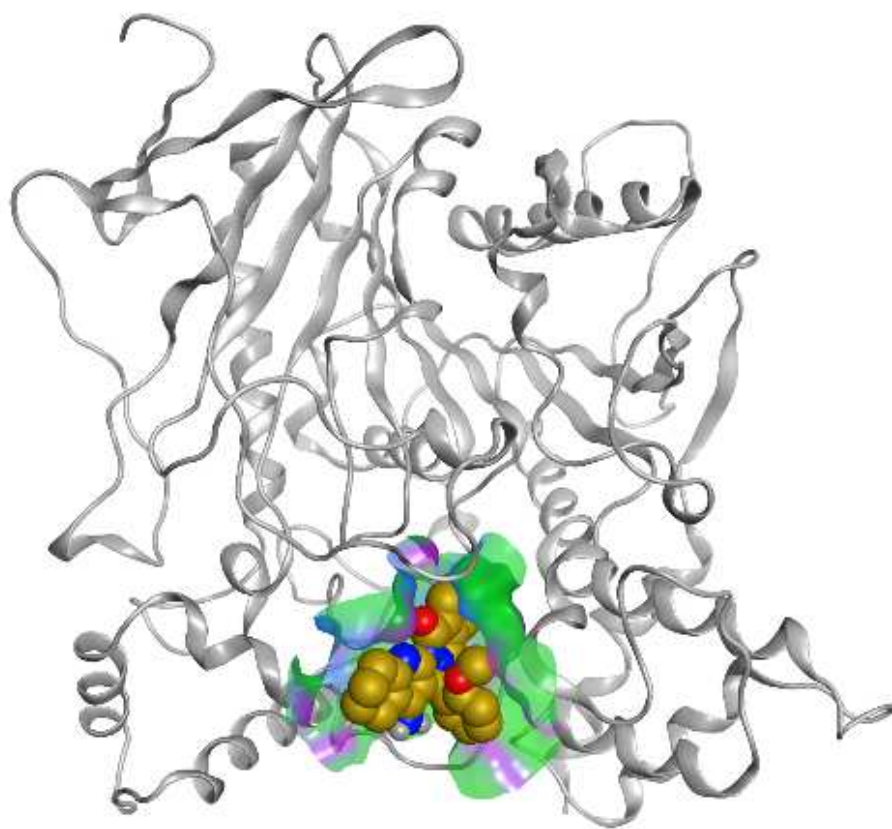
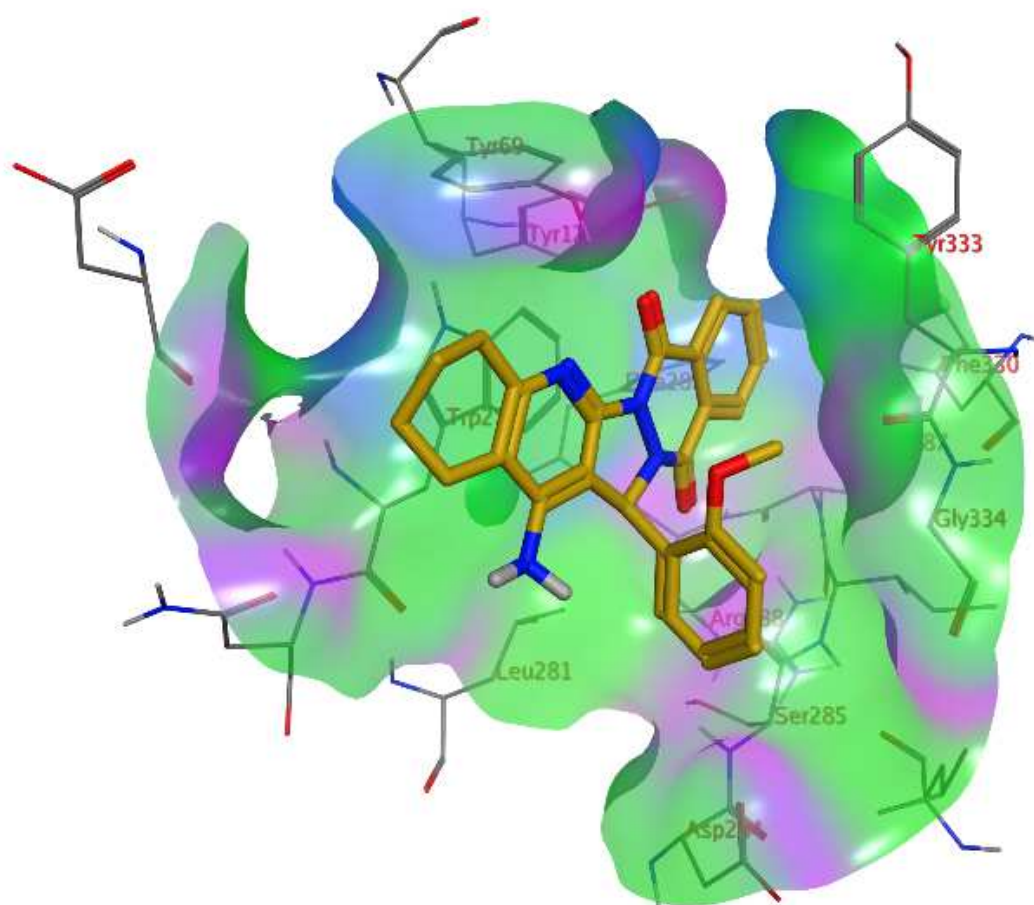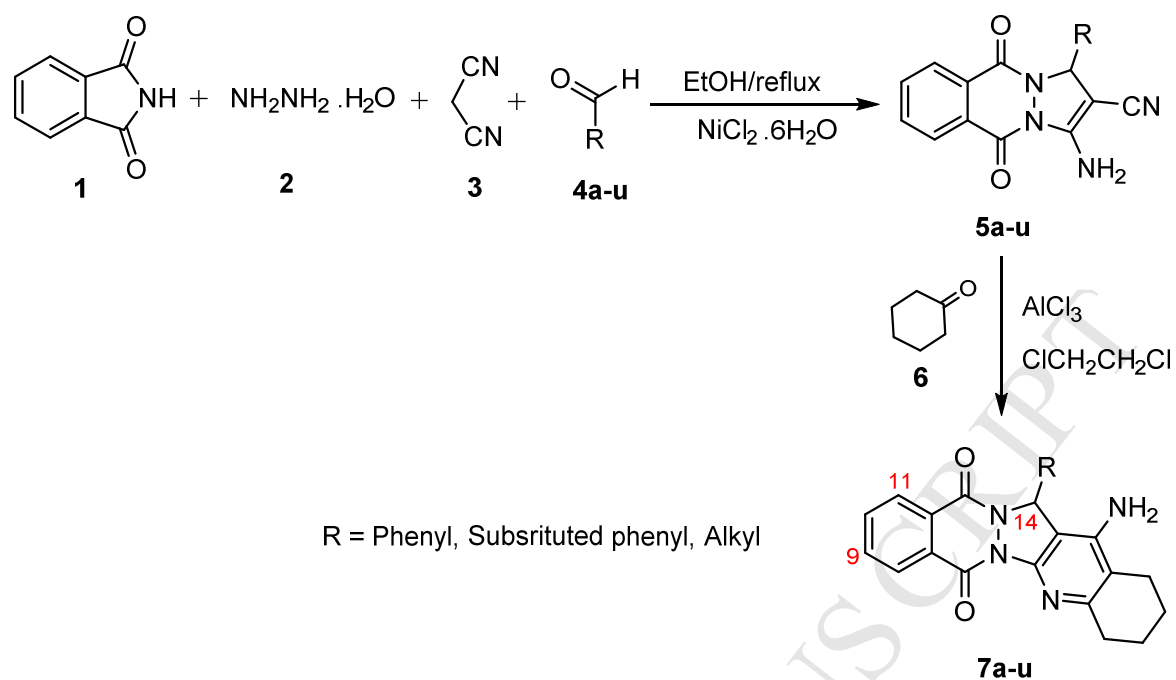**Figure 4.** The proposed orientation of compound **7l** in the AChE active site.

Figure 5. The binding mode of compound **7l** in the active site of AChE.

Scheme 1. Synthesis of compounds **7a-u**.

Highlights

- A series of tacrine-modified compounds were synthesized as potent AChE inhibitors.

- Several compounds had high anti-AChE activity at nano-molar level.

- The 2-methoxyphenyl derivative **7l** was 7-fold more potent than tacrine.

- Compound **7l** had lower toxicity on HepG2 cells compared to tacrine.

- Compound **7l** had significant neuroprotective and Aβ aggregation inhibitory activities.